



## Equatorial Electrojet and electron density over Southeast Asian Region during moderate solar activity condition

Saeed Abioye Bello<sup>a</sup>, Nurul Shazana Abdul Hamid<sup>b,c\*</sup>, Mardina Abdullah<sup>d</sup>, Akimasa Yoshikawa<sup>e,f</sup>, Kornyanat Hozumi<sup>g</sup> & Takuya Tsugawa<sup>g</sup>

<sup>a</sup>Department of Physics, University of Ilorin, Ilorin South 240003, Nigeria

<sup>b</sup>Department of Applied Physics, Universiti Kebangsaan Malaysia, Bangi, Selangor 43600, Malaysia

<sup>c</sup>Space Science Centre (ANGKASA), Institute of Climate Changes, Universiti Kebangsaan Malaysia, Bangi, Selangor 43600, Malaysia

<sup>d</sup>Department of Electrical, Electronic and Systems Engineering, Universiti Kebangsaan Malaysia, Bangi, Selangor 43600, Malaysia

<sup>e</sup>Department of Earth and Planetary Sciences, 33 Kyushu University, 6-10-1 Hakozaki, Higashi-ku, Fukuoka 812-8581, Japan

<sup>f</sup>International Center for Space Weather Science and Education, Kyushu University, 53, 6-10-1 Hakozaki, Higashi-ku, Fukuoka 812-8581, Japan

<sup>g</sup>National Institute of Information and Communications Technology, 4-2-1 Nukui-Kita, Koganei, Tokyo 184-8795, Japan

*Received: 10 July 2019; Accepted: 30 January 2021*

The study presents a simultaneous variation of equatorial electrojet (EEJ) current and the ionospheric F2-layer maximum electron density (NmF2) during geomagnetic quiet days and moderate solar conditions (solar radio flux,  $F_{10.7} \approx 120$  sfu). The geomagnetic measurements at Kotatobang (KTB) and Langkawi (LKW) stations have been used to estimate the magnetic daily variation in H-component and in deriving EEJ. The NmF2 data set is from Frequency Modulation Continuous Wave (FM-CW), an analogue ionosonde located at the KTB station. The study examines both the diurnal and seasonal variation in EEJ and the corresponding effect on the measured NmF2. The results obtained show that the derived EEJ at LKW shows a daytime peak which coincides with the period NmF2 measurement at KTB station depleted to a daytime low value. The role of EEJ at the LKW station correlates poorly with the NmF2 at KTB in which their correlation coefficient ( $r$ ) is in the range of 0.02 to 0.04 for equinox, summer and winter, respectively. However, an  $r$ -value of 0.33 was observed when the whole data set for the year 2012 was considered. The poor correlation coefficient between derived EEJ and NmF2 measured at KTB during the moderate solar condition suggest that EEJ has little or no influence on the prevailing ionospheric condition at a low latitude station located outside the EEJ strip.

**Keywords:** Ionosphere, Equatorial electrojet, Ionospheric electron density, Frequency Modulation Continuous Wave (FM-CW)

### 1 Introduction

The variations of ionospheric electron density around the geomagnetic dip equator are mostly related to the equatorial electrojet (EEJ) current system. The EEJ is a daytime enhanced ribbon of current flowing eastward in the dynamo E-region height (100 to 120 km) and confined between  $\pm 3^\circ$  latitude of the dip equator<sup>1</sup>. In the build-up of the EEJ after sunrise, the E-region dynamo is driven by the worldwide solar wind across the magnetic field which creates east-west electric field (E) that is transported to the ionospheric F-region height along with the conducting geomagnetic field lines<sup>2</sup>. Subsequently, the E field over the geomagnetic equator is perpendicular to the geomagnetic field (B) resulting to

an upward  $E \times B$  plasma drift that is responsible for the occurrences of the equatorial ionospheric anomaly (EIA). The uplifted plasma (also known as the fountain process) at the F-region altitude near the dip equator then diffuses along with the B field. The direction of the plasma diffusion is downward and moves towards the higher altitude under the influence of gravity, pressure gradient and the decreasing ion-neutral drag force<sup>3</sup>. This fountain process causes the observed depletion (trough) of electron density around the magnetic dip equator and thus producing two peaks (crest) on both sides of the geomagnetic equator ( $\pm 15$  to  $20^\circ$ ).

Over the dip equator, the fountain process is driven by the  $E \times B$  plasma drift being controlled by EEJ<sup>4</sup>. Thus, the study of EEJ and EIA phenomena is important in examining the electron redistribution

\*Corresponding author (E-mail: shazana.ukm@gmail.com)

over the ionospheric equatorial and low latitude region. The plausible role of EEJ modulating the daytime vertical drift has been observed to have strong correlation coefficient<sup>2,5,6,7</sup>, thus, justifying related primary causes of EIA and EEJ phenomena. Previous, studies have reported a significant relationship between the strength of EIA and integrated EEJ (IEEJ) at the Indian and Brazilian sectors<sup>4</sup>. Likewise, the influence of EEJ on the observed maximum electron density, NmF2 measured at Ilorin station (Geographic coordinates: 8.50°N, 4.68°E) shows some lag in-between the peak of EEJ and the daytime trough in NmF2<sup>8</sup>. The observed lag is related to the time of maximization of the EIA that is a function of the maximum electric field.

The present study aims to examine the contribution of EEJ to the diurnal variation of NmF2 observed at a station within the EIA zone but off the EEJ strip. This study uses the simultaneous measurement of geomagnetic H-component data and ionosonde measurement during geomagnetic quiet and moderate solar conditions.

## 2 Materials and Methods

We have used ionospheric data from an analogue ionosonde of the type FM-CW located at Kotatobang (KTB) in Indonesia (Geographic coordinates: 0.20°S, 100.32°E). The KTB station is among the ionosonde stations in the South-East Asia Low-latitude Ionospheric Network (SEALION). The FM-CW ionosonde has been well described in the study of Nozaki<sup>9</sup>. The ionospheric NmF2 values are calculated using the relationship with the critical frequency of ionospheric F-layer (foF2).

$$NmF2 = 1.24 \times (foF2)^2 \times 10^{10} \quad \dots (1)$$

where, NmF2 is in  $m^{-3}$  and foF2 is in MHz. The FM-CW ionosonde works by transmitting high frequency (HF) radio signal within 1 to 30 MHz. The time delay of the reflected radio signals trace was recorded in what is known as an ionogram. The foF2 parameter was manually scaled from the ionogram data set and NmF2 was then calculated using the formula given in Eq. (1). The extraction of the foF2 values on the ionogram data set was done using the SEAIONO software developed by the Space Science Center (ANGKASA), Universiti Kebangsaan Malaysia<sup>10</sup>.

Furthermore, the geomagnetic H-component data used in calculating the equatorial electrojet (EEJ) current was obtained from a ground magnetometer

installed at Kotatobang (KTB) and Langkawi (LKW) stations. The H-component measurement from these stations (KTB and LKW) are magnetic records from the Magnetic Data Acquisition System (MAGDAS)<sup>11</sup>. The LKW (Geographic coordinates: 6.30°N, 99.78°E) station is found around the dip equator and accordingly is within the EEJ strip. However, the KTB station was off the magnetic dip equator and is not located in the EEJ zone. The locations of these stations in that way satisfy the pair-station method of estimating EEJ current<sup>12</sup>. In the two-station method, EEJ can be calculated by subtracting the quiet daily (Sq) variation of H-component, Sq(H) measured close to the dip equator and that off the dip equator.

The Sq (H) was calculated by deducting the daily baseline value from the hourly values of the measured H-component. The daily baseline value was defined as the average of the night time adjoining hours of the geomagnetic H-component about the local time 0000h, 0100h, 2200h and 2300h respectively<sup>13</sup>. The subtraction of the baseline values from the H-component records was necessary because of the ionospheric conductivity at dynamo E-region altitudes diminishes during the nighttime<sup>14</sup>. Thus, the expression for calculating the quiet daily variation of geomagnetic H-component Sq(H) is given as:

$$\Delta H = H_{LT} - BV \quad \dots (2)$$

where,  $\Delta H$  represents Sq(H),  $H_{LT}$  indicates the hourly values of the geomagnetic H-component and the BV stands for baseline values.

At a location closer to the magnetic dip equator, the calculated  $\Delta H$  includes both components of EEJ current and the planetary Sq current effects. One way of isolating the EEJ current from the total Sq current is by adopting a pair-station method<sup>5,7,15,16</sup>. The method entails considering a pair of the station, with one located close to the dip equator and the other outside the equator. For this study, the calculated  $\Delta H$  at KTB station ( $\Delta H_{KTB}$ ) is subtracted from  $\Delta H$  at LKW station ( $\Delta H_{LKW}$ ) to give the overhead EEJ at the LKW station ( $EEJ_{LKW}$ ).

$$EEJ_{LKW} = \Delta H_{LKW} - \Delta H_{KTB} \quad \dots (3)$$

Figure 1 for example shows the quiet day  $\Delta H$  values at both the LKW and KTB stations. The EEJ causes an increment in the magnitude of the observed geomagnetic H-component measured within the  $\pm 3^\circ$  of the dip equator<sup>7</sup>. This enhancement is manifested in the magnitude of  $\Delta H_{LKW}$  which is seen to be higher than

$\Delta H_{KTB}$ . The noon-time maximums were about 122 nT at the LKW station and 66 nT at the KTB station. The location of the two stations was responsible for the observed differences in the noon time maximum values of  $\Delta H_{LKW}$  and  $\Delta H_{KTB}$ . Also, the magnitude of  $\Delta H_{LKW}$  has both the effect of EEJ current and the total Sq current. The isolated effect of EEJ current,  $EEJ_{LKW}$  (the blue dash curve) was calculated after subtracting  $\Delta H_{KTB}$  (black square dotted line) from  $\Delta H_{LKW}$  (red thick line).

The simultaneous variation of NmF2 and geomagnetic H-component are studied during the year 2012. The 27-day averaged solar radio flux,  $F_{10.7}$  for the study period is 120 sfu. The term *sfu* means the solar flux unit ( $10^{-22} \cdot m^{-2} \cdot Hz^{-1}$ ) which describes the ambient solar condition. In each month, ten days with geomagnetic quiet conditions were used for the study. These quiet days are period with Ap index less than

26 and Kp index less than 3 and are retrieved from the World Data Center (WDC) for Geomagnetism, Kyoto via <http://wdc.kugi.kyoto-u.ac.jp/qddays/index.html>. The data set are then grouped into astronomical/Lloyd's seasonal calcification<sup>4</sup> namely equinox (March-April and September-October), summer (northern summer: May-August; southern summer: January-February and November-December) and winter (northern winter: January-February and November-December; southern winter: May-August).

### 3 Results and Discussion

The diurnal variation of geomagnetic H-component ( $\Delta H$ ) during geomagnetic quiet conditions in the year 2012 is given in Fig. 2. The thin grey lines give the day-to-day values of  $\Delta H$  and the thick line with the error bar gives the seasonal averages (the error bar is calculated from the standard deviation). In general, the diurnal variation of  $\Delta H$  is highest at noon. The values of  $\Delta H$  are about the baseline level 0000h to 0700h LT during the morning and 1800h to 2300h LT. For all the seasons, there is both diurnal and seasonal variation observed. The values of  $\Delta H$  increase from 0800h LT in all the seasons to reach a daytime peak at 1200h LT. The daytime peak in  $\Delta H$  during equinox is higher than the other seasons with an average value of 124 nT in equinox (Fig. 2a), 97 nT in summer (Fig. 2b), and 88 nT in winter (Fig. 2c). The values of  $\Delta H$  gradually reduce from 1300h LT towards the night. The observed negative values of  $\Delta H$  in the range of -5 to -30 nT are due to the effect of Counter Electrojet (CEJ).

Figure 3 shows the daytime variation of EEJ during the geomagnetic quiet periods in the year 2012. The grey lines and the blue curve with error bar depict the daily values ( $\Delta H_{EEJ}$ ) and the seasonal averages of EEJ

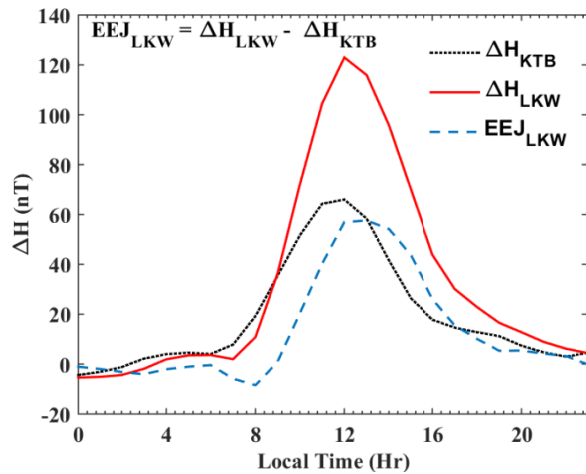


Fig. 1 — The average measured values of geomagnetic H-component at a station near (LKW) and outside the dip equator (KTB) on the 29<sup>th</sup> to 31<sup>st</sup> March 2012.

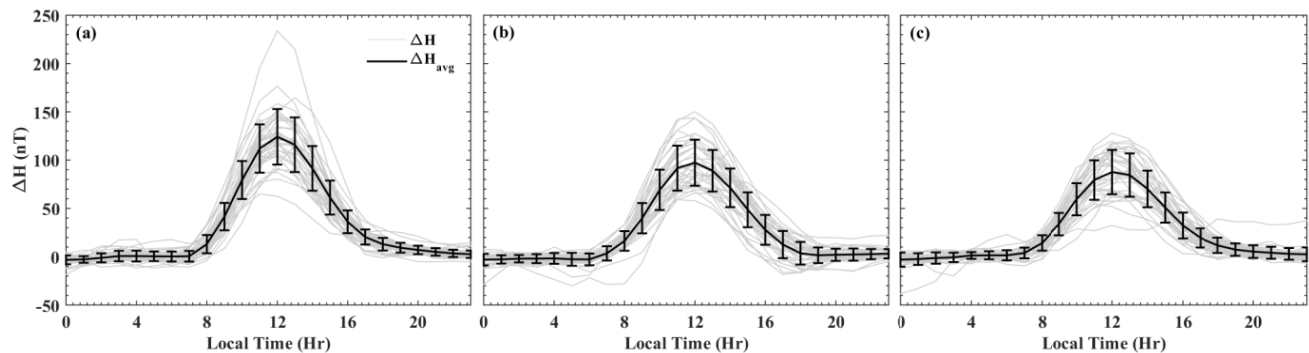


Fig. 2 — Diurnal seasonal variation  $\Delta H$  at the Langkawi (LKW) station during (a) equinox, (b) summer, and (c) winter for the year 2012. The grey lines are the daily value of  $\Delta H$ , the black thick line represents the seasonal averages and the error bar is the standard deviation of EEJ current.

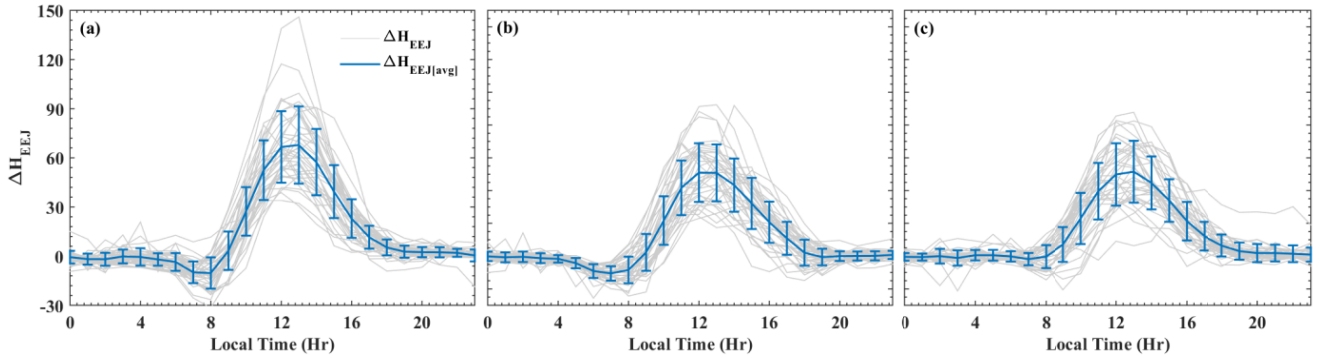


Fig. 3 — Seasonal variation of EEJ current at the Langkawi (LKW) station during (a) equinox, (b) summer, and (c) winter for the year 2012. The grey lines are the daily value of EEJ current, the blue thick line represents the seasonal averages and the error bar is the standard deviation of EEJ current.

( $\Delta H_{EEJ,avg}$ ) at the LKW station respectively. The intensity of EEJ during the daytime (0800h to 1600h LT) is higher than the night time values. The values EEJ gradually increased from the baseline level at about 0800h LT to a maximum value at noontime. Generally, an observed daily variation in EEJ was found to be significant in all the seasons.

The abnormal decrease in the magnitude of  $\Delta H$  (CEJ) is predominantly observed during the morning. The decrease in the magnitude of  $\Delta H$  is because of the reversal of the current direction<sup>4</sup>. Moreover, the maximum seasonal average value of EEJ during local noon in equinox is about 68 nT and 50 nT in summer and winter.

Figure 4 shows the day-to-day relationship between  $\Delta H$  and the calculated  $\Delta H_{EEJ}$  at the LKW station for geomagnetic quiet days during the year 2012. A good correlation ( $r$ ) is seen between  $\Delta H$  and the intensity of  $\Delta H_{EEJ}$  with  $r$ -value equal to 0.93. Previous reports suggest a significant relationship between the diurnal variation of geomagnetic H-component and EEJ<sup>17</sup>. However, days in which  $\Delta H$  and  $\Delta H_{EEJ}$  show no trend can be attributed to the abnormal decrease in the magnitude of geomagnetic H-component over the dip equator. The observed phenomenon is known as Counter Electrojet (CEJ) and has been observed in both  $\Delta H$  and EEJ. CEJ is found when the magnitude of  $\Delta H$  and EEJ is below the baseline values.

The simultaneous variation of average values of EEJ and NmF2 are shown in Fig. 5 for different seasons. From Fig. 5 (a), the variations of NmF2 during equinox increase from  $3 \times 10^{11} m^{-3}$  at 0600h LT to  $15 \times 10^{11} m^{-3}$  between 0900h to 1000h LT (pre-noon peak). Subsequently, the values of NmF2 decrease at the noontime to  $13 \times 10^{11} m^{-3}$ .

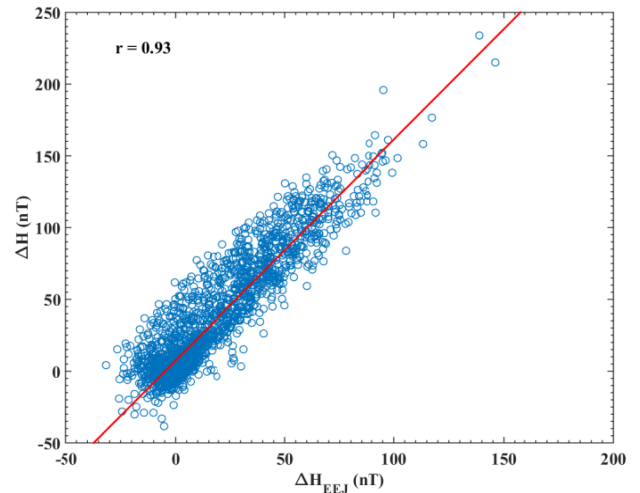


Fig. 4 — Scatter plot of geomagnetic H-component ( $\Delta H$ ) against EEJ current at the Langkawi (LKW) station during the year 2012.

The decrease in NmF2 during this period is due to the  $E \times B$  drift causing the plasma to move across the geomagnetic dip equator at the altitudinal range of F2 layer plus the resultant effect of the changes in pressure and gravity<sup>8</sup>. The other peak observed in NmF2 is found at 1700h LT with a value around  $18 \times 10^{11} m^{-3}$  and later decrease between the periods of 1800h to 2000h LT. An abrupt but short leave rise in NmF2 is observed at 2200h LT and decreases continuously afterwards throughout the night time until 0500h LT. Meanwhile, EEJ during the morning and night time (1900h to 0600h LT) is about the baseline level. Furthermore, the decrease in EEJ (CEJ), -10 nT at 0800h LT corresponds to the observed pre-noon peak in NmF2. There was no lag in-between the time EEJ peak was observed and the period in which plasma is drifted. Likewise, the

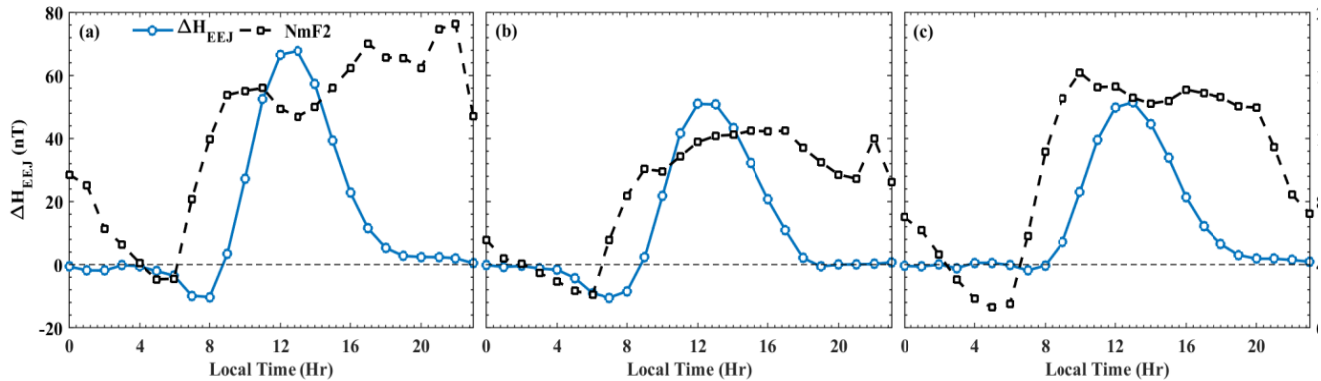


Fig. 5 — The simultaneous variation of EEJ current (blue line), and NmF2 (brown line) at the Langkawi (LKW) station during the year 2012 for (a) equinox, (b) summer, and (c) winter.

daytime peak in EEJ at 68 nT coincide with the daytime depression in the magnitude of NmF2. Successively, the value of EEJ is at baseline after sunset and show no relationship with the evening peaks observed in NmF2.

Figure 5(b) shows the variation of NmF2 and EEJ during summer. It is worthy to note that EEJ was at northern summer (LKW station) and NmF2 was at southern summer (KTB station). The variation of NmF2 during the pre-sunrise period has a similar trend with that of the equinox. NmF2 was seen to increase from  $2 \times 10^{11} m^{-3}$  at 0600h LT and reached a pre-noon peak ( $10 \times 10^{11} m^{-3}$ ) at 0900h LT. However, there is no significant daytime reduction in the values of NmF2 during southern summer. Nonetheless, EEJ intensity during the daytime is stronger than night time. Also, the observed CEJ (-10 nT) around 0700h LT followed the observed pre-noon peak in NmF2. There is no clear relationship between EEJ and NmF2 during the day and night time.

Figure 5(c) shows the variation of the seasonal diurnal average values of EEJ and NmF2 during winter. Similarly, the EEJ describes by data of LKW station in the northern hemisphere and NmF2 is data from KTB station in the southern hemisphere. The variation of NmF2 is having a similar pattern with that of equinox showing daytime depression in NmF2 coinciding with the peak of EEJ. However, NmF2 during winter has two distinct peaks, one at 1000h LT ( $16 \times 10^{11} m^{-3}$ ) and the other at 1600h LT ( $15 \times 10^{11} m^{-3}$ ). The daytime value of NmF2 is higher during winter than summer indicating a winter anomaly. Yet, the magnitude of NmF2 during the night time is lower than the other seasons. The

variation in EEJ, on the other hand, does not exhibit CEJ as compared to the rest of the other seasons. Also, EEJ intensity during winter is lower than equinox and summer.

To establish the role of EEJ on the variation on NmF2, the correlation coefficient is calculated using a daytime value within the period of 0700h to 1200h LT. These periods describe the rise (fall) of EEJ and NmF2, which in turns should reveal the contribution of EEJ (if any) of the observed changes in NmF2.

Figure 6 shows the correlation coefficient between EEJ and NmF2 are 0.02, 0.03 and 0.04 for equinox, summer and winter respectively. Likewise, the correlation coefficient for all the daytime values of EEJ and NmF2 during geomagnetic quiet conditions in 2012 is 0.33. The result of the analysis shows that role of the derived EEJ at the LKW station correlates poorly with the measured NmF2 at the KTB station during the moderate solar condition. This suggests that EEJ at LKW has no contribution to the observed variability of NmF2 at the KTB station. The results of this study are supported by previous findings obtained at the Jicamarca station, Peru, Brazil<sup>18</sup>. They attributed the poor correlation between EEJ and NmF2 during the moderate solar activity condition to the contribution of EEJ and the directions of the electric and magnetic fields during the daytime plasma drift that is responsible for the reduction of electron density over the dip equator. The overall correlation coefficient result is may as well be due to the location of the KTB station being outside the EEJ region. Hence, the effect of EEJ on the electron distribution is significant at the station close to the magnetic equator within the  $\pm 3^\circ$  latitude,

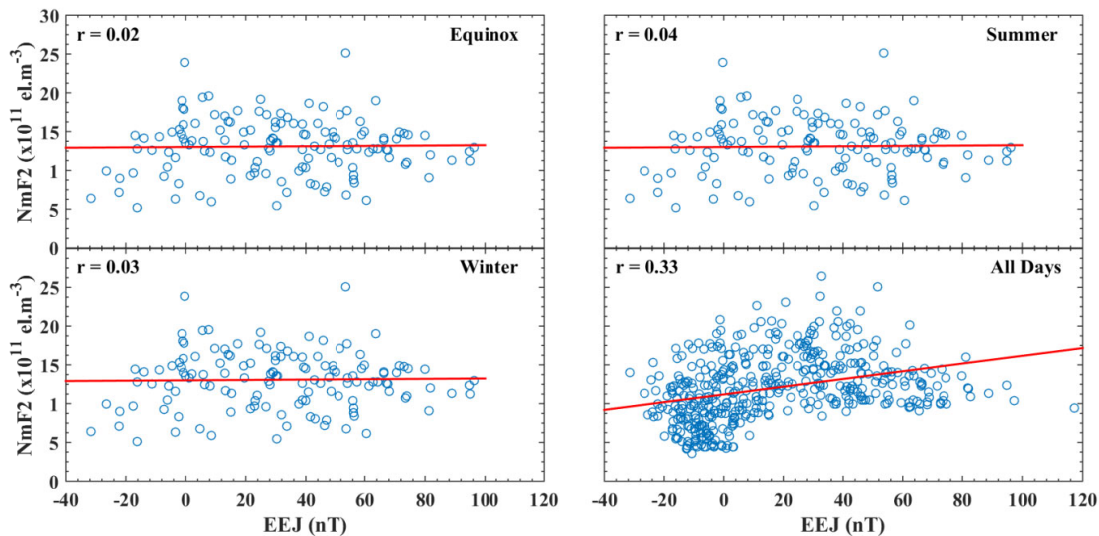


Fig. 6 — The scatter plots for NmF2 values as a function of EEJ intensity during geomagnetic quiet conditions in the year 2012.

where the EEJ current flow is under the right solar conditions.

#### 4 Conclusion

The variability of EEJ and NmF2 are simultaneously studied using geomagnetic and ionospheric data from KTB (southern hemisphere) and LKW (northern hemisphere) stations. The ground-based magnetometer measurements during moderate solar conditions (2012) have been used to calculate EEJ values. EEJ variations in all the seasons show significant day-to-day variability, which has a high intensity in equinox than the rest of the other season. The magnitude of the diurnal changes in geomagnetic H-component together with the isolated effect of EEJ have values during the daytime higher than night time and both have a strong correlation coefficient ( $r = 0.93$ ). The study demonstrates that the daytime maximum intensity in EEJ coincides with the daytime depression in NmF2 attributed to the  $E \times B$  drift of plasma. The overall correlation coefficient between EEJ and NmF2 at LKW and KTB is poor. The result obtained has been attributed to the combined effect of the moderate solar activity conditions dominating the observed relationship between the two parameters and the confinement of EEJ within  $\pm 3^\circ$  dip equator. Since KTB station is located at  $-10^\circ$  geomagnetic latitude, as a consequence, EEJ has little or no significant influence on the observed variation in NmF2 outside the EEJ strip during moderate solar conditions.

#### Acknowledgement

The ionogram data from Kotatobang station was provided by the Space Science Centre (LAPAN) and the National Institute of Information and Communications Technology (NICT). The magnetometer data from Langkawi and Kotatobang stations was provided by the MAGDAS group, Japan. The authors are grateful to these institutions for providing the data used in this study. The radio solar flux index ( $F_{10.7}$ ) data were downloaded from the Omni Web. The geomagnetic Ap and Kp indexes were obtained from the World Data Centre (WDC) for Geomagnetism, Kyoto. This work was supported by the Fundamental Research Grant Scheme (FRGS) FRGS/1/2018/STG02/UKM/02/3 from the Ministry of Higher Education, Malaysia.

#### References

- 1 Hamid N S A, Liu H, Uozumi T, & Yoshikawa A, *Earth Planets Space*, 67 (2015) 205.
- 2 Sreeja V, Devasia C, Ravindran S, & Pant T K, *Ann Geophys*, 27 (2009) 4229.
- 3 Maruyama T, Uemoto J, Ishii M, Tsugawa T, Supnithi P, & Komolmis T, *J Geophys Res Space Phys*, 119 (2014) 1059.
- 4 Venkatesh K, Fagundes P, Prasad D, Denardini C, Abreu A, Jesus R, & Gende M, *J Geophys Res Space Phys*, 120 (2015).
- 5 Anderson D, Anghel A, Yumoto K, Ishitsuka M, & Kudeki E, *Geophys Res Lett*, 29 (2002) 1596.
- 6 Devi P S, & Unnikrishnan K, *Adv Space Res*, 53 (2014) 752.
- 7 Yizengaw E, Moldwin M, Zesta E, Biouele C, Damtie B, Mebrahtu A, Rabiou B, Valladares C, & Stoneback R A, *Ann Geophys*, 32 (2014) 231.

- 8 Adebessin B, Adeniyi J, Adimula I, Reinisch B, & Yumoto K, *Adv Space Res*, 52(2013) 791.
- 9 Nozaki K, *Journal of NICT*, 56 (2009) 287.
- 10 Bello S A, Abdullah M, Hamid NSA, & Yokoyama A, *J Phys Conf Ser*, 1152 (2019) 012015.
- 11 Yumoto K, & CPMN Group, *Earth Planets Space*, 53 (2001) 981.
- 12 Hamid NSA , Liu H, Uozumi T, Yumoto K, Veenadhari B, Yoshikawa A, & Sanchez, J A, *Earth Planets Space*, 66 (2014) 146.
- 13 Bello S A, Abdullah M, Hamid N S A, Yoshikaw A, & Olawepo A, *Adv Space Res*, 60 (2017) 307.
- 14 Yamazaki Y, Richmond A, Maute A, Liu H L, Pedatella N, & Sassi F, *J Geophys Res Space Phys*, 119 (2014) 6966.
- 15 Hamid N S A, Liu H, Uozumi T, & Yumoto K, *Antarct Rec*, 57 (2013) 329.
- 16 Benaissa M, Berguig M, Doumbia V, & Bouraoui S, *Africa, Arab J Geosc*, 10 (2017) 329.
- 17 Yamazaki Y, Yumoto K, Uozumi T, Abe S, Cardinal M, Mcnamara D, Marshall R, Shevtsov B, & Solovyev S, *J Geophys Res Space Phys*, 115 (2010) A09319.
- 18 Bello S A, Abdullah M, Hamid N S A, Reinisch B W, Yoshikawa A, & Fujimoto A, *Earth Space Sci*, 6 (2019) 617.